Fundamental Properties and Origin of the High-T_c Cuprate Superconductors: Development of Concepts

A. Bechlaghem*

Faculté des Sciences de la Nature et de la Vie, Université d'Oran, Es-sénia, 31100, Algeria

Abstract: After a review of the fundamental properties of the high-T_c cuprate superconductors, we evaluate and study the major parameters of these compounds. In this approach, we consider the attractive interaction is due to the phonons at low temperature, but at high temperature it is related to the magnetic excitations. Analytical expressions for the coherence length ξ, the isotope coefficient α and the superconducting gap ratio $R = 2\Delta(0)/k_B T_c$ are obtained for the case where the Fermi level is close to the van Hove singularity. This model explains simultaneously high T_c, large gap energy $\Delta(0)$, short coherence length ξ and small values of the isotope coefficient α. Our theoretical values are in a good agreement with experimental results.

Keywords: Electron-phonon interaction, Magnetic excitations, Van Hove singularity, Gap energy, Pseudogap, Coherence length, Isotope coefficient, Superconducting gap ratio.

1. INTRODUCTION

Physics of high-T_c superconductors has been a very interesting domain during the period following the discovery of high-temperature superconductivity by Bednorz and Müller in 1986 [1]. They discovered the superconductivity in lanthanum compound $La_{2-x}M_xCuO_4$ (M is an alkaline-earth metal: M = Ba, Sr or Ca) with $T_c^{\max} \approx 30$ K. Since this discovery, other compounds are discovered and the critical temperature has reached values of the order of 135 K. During this period, there is an intense research both experimentally and theoreticcally to understand the fundamental mechanism of superconductivity in these compounds. There are many unsolved problems both in the normal and superconducting states. There are five types of materials of the hole-doped cuprates:

- lanthanum compound $La_{2-x}M_xCuO_4$ with $T_c^{\max}$ = 38 - 39 K for $x \approx 0.15 - 0.16$. For $x = 0$, this compound is antiferromagnetic (AF) insulator. This AF disappears for $x > 0.03$, while superconductivity appears for $x > 0.06$ and decreases to zero for $x = 0.27$ (Figure **1**);

- yttrium compound $YBa_2Cu_3O_{6+x}$ with $T_c^{\max}$ = 91 - 93 K for $x = 0.9$. This compound is AF insulator for $x = 0$. $T_c(x)$ increases beyond $x = 0.4$ up to $x = 0.6$ with a second increase up to $x = 0.9$ (Figure **2**);

- bismuth compounds $Bi_mSr_2Ca_{n-1}Cu_nO_{2n+m+2+x}$ $(m2(n-1)n, n = 2,3)$: the compound Bi-2212 *i.e* $Bi_2Sr_2CaCu_2O_8$ with $T_c^{\max}$ = 85 – 86 K and Bi-2223 *i.e* $Bi_2Sr_2Ca_2Cu_3O_{10}$ with $T_c^{\max}$ = 110 K;

- thallium compounds $Tl_mBa_2Ca_{n-1}Cu_{n-}O_{2n+m+2}$ $(m2(n-1)n, n = 2,3)$: the compound Th-2212 with $T_c^{\max}$ = 100 K and Th-2223 with $T_c^{\max}$ = 125 K;

- mercury compounds $HgBa_2Ca_{n-1}Cu_nO_{2n+x+2}$ $(Hg-12(n-1)n, n = 1,2,3)$. Samples of optimally doped Hg-1201, Hg-1212, and Hg-1223 have critical temperature $T_c^{\max} = 96$ K, 123 K and 135 K respectively.

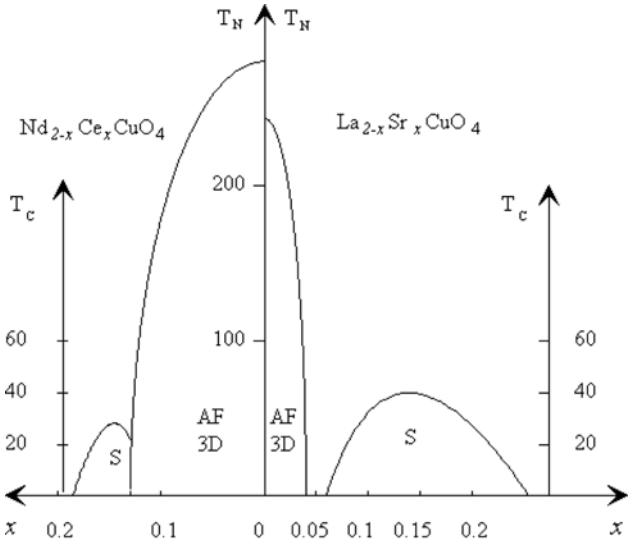

Figure 1: Phase diagrams of lanthanum compound $La_{2-x}Sr_xCuO_4$ for $0 \le x \le 0.27$ and neodymium compound $Nd_{2-x}Ce_xCuO_4$ for $0 \le x \le 0.2$ [37].

These new compounds differ from the conventional superconductors in various ways. All the high-T_c cuprate superconductors have CuO_2 planes playing a

*Address correspondence to author at the Faculté des Sciences de la Nature et de la Vie, Université d'Oran, Es-sénia, 31100, Algeria;
E-mail: alibechlaghem@yahoo.fr

E-ISSN: 2408-977X/14 © 2014 Cosmos Scholars Publishing House

fundamental role both in the normal and superconducting states. These new superconductors are doped materials, with T_c strongly depending on the carrier concentration x. In the absence of doping, the CuO_2 plane has strong antiferrmagnetic correlation and the insulating antiferroagnetic state is converted into a metallic paramagnetic one with doping [2]. The superconducting transition temperature $T_c(x)$ increases with doping and reaches its maximum at optimum doping x_{op}. The overdoped state of the high-T_c oxides is characterized by a decrease in T_c. An additional increase in hole doping x, leads to a total suppression in superconductivity. It has been suggested that there is an universal relation between T_c and the hole concentration x. The superconducting transition temperature can be described by the empirical formula: $T_c(x)/T_c^{\max} = 1-((x_{op}-x)/x_l)^2$ where x_{op} the optimum doping and x_l the width of the parabola [3-5]. The parabolic form of the curve obtained from this formula, seams universal for all the cuprates. In the underdoped region, the cuprate superconductors are characterized by the opening of a pseudogap. This phenomenon can be reconciled with the van Hove singularity [4]. In the low doping regime, the pseudogap $\Delta_{pg}(x)$ is large compared to the superconducting gap $\Delta_{sg}(x)$ [6]. When the hole concentration x increases the pseudogap decreases while the superconducting gap increases. At optimum doping $\Delta_{sg}(x)$ is maximum and $\Delta_{pg}(x)$ is suppressed to zero. The SC gap can be described by the empirical formula deduced from $T_c(x)$: $\Delta_{sg}(x)/\Delta_{sg}^{\max} = 1-((x_{op}-x)/x_l)^2$ and the pseudogap can be expressed as $\Delta_{pg}(x)/\Delta_{pg}^{\max} = (1-x/x_{op})$ [7]. The pseudogag increases weakly with the temperature T while the SC gap decreases with T. The total gap $\Delta(T) = \sqrt{\Delta_{sg}^2(T)+\Delta_{pg}^2(T)}$ is nearly constant and consistent with experimental observations [8]. The pseudogap $\Delta_{pg}(T)$ reaches its maximum at $T > T_c$. From its maximum, $\Delta_{pg}(T)$ decreases with T and it is suppressed at pseudogap critical temperature T^*.

At low temperature, the total gap becomes a pure SC gap, but at high temperature it is a pure pseudogap ($T_c < T < T^*$), and at intermediate temperatures the gap has two contributions, one form the superconducting gap and the other form the pseudogap [6, 9].

In conventional superconductors, pairing of charge carriers and superfluidity of Cooper pairs occur simultaneously at $T^* = T_c$. In cuprate superconductors, the pairing of charge carriers may be occur at high pseudogap temperature T^* than T_c at which the preformed Cooper pairs condense in a superconducting state [10].

Now we list some of number of electronic properties which are anomalous from the standard point of BCS behavior. These anomalous electronic properties include: (a) extremely short in plane coherence lengths have been determined for some of the cuprate superconductors: about 16 Å for yttrium compound $YBa_2Cu_3O_7$ [11, 12], 13.6 Å for thallium compound Tl-2223 [13], 9.7 Å for Bi-2223 and 9 ± 1 Å for Bi-2212 [14], (b) large penetration depth λ which with (a) causes type-II behavior with $\kappa = \lambda_L/\xi > 10$, (c) low charge carriers density n, (d) an enhanced effective mass m^*, (e) small isotope coefficient α: in general this coefficient is greater than zero but it is significantly smaller than the BCS value $\alpha = 0.5$ [15-21]. For instance the isotope coefficient is $\approx 0.06-0.09$ in $La_{1.85}Sr_{0.15}CuO_4$ with $T_c^{\max} \approx 38$ K; $\alpha \approx 0.02-0.03$ in $YBa_2Cu_3O_7$ with $T_c^{\max} \approx 92$ K; $\alpha \approx 0.03-0.05$ in $Bi_2Sr_2CaCu_2O_8$ with $T_c^{\max} \approx 86$ K; $\alpha \approx 0.03$ and even negative ($\alpha = -0.013$) in $Bi_2Sr_2Ca_2Cu_3O_{10}$ with $T_c^{\max} \approx 110$ K. The deviation of α from the BCS value remains an open question, (**f**) large value of the superconducting gap ratio $R = 2\Delta(0)/k_B T_c$: this parameter has the magnitude ≈ 3.53 for the conventional superconductors, but it is much larger being $\approx 5-13$ for the cuprate superconductors [22-30]. A break-junction tunneling study of the single crystal $La_{1.85}Sr_{0.15}CuO_4$ has found a superconducting gap ratio of 8.9 ± 0.2 [22]. Experimental results show that this ratio is 10.2 ± 0.4 for yttrium compound $YBa_2Cu_3O_{6+x}$ and 10 for bismuth compounds [23]. Other experimental results show that for optimally doped Hg-1201, Hg-1212 and Hg-1223, the superconducting gap ratios are respectively 7.9, 9.5 and 13 [24]. The problem of the small isotope coefficient and the large ratio R are still not understood. Various theories, based on electronic as well as phonon based interactions, have been proposed to explain different properties of the high-T_c superconductors.

In this work we develop the Kuruhara model in the van Hove scenario [31]. We consider the attractive interaction is due to the phonons at low temperature but at high temperature it is related to the magnetic excitations. We discuss several properties of these compounds. To understand the electron pairing mechanism responsible for superconductivity in high-T_c superconductors, it is necessary to have a clear picture of the magnetic and electronic structure of these compounds.

2. MAGNETIC PROPERTIES

The cuprate superconductors such $La_{2-x}Sr_xCuO_4$ and $YBa_2Cu_3O_{6+x}$ are antiferromagnetic insulators in low doping regime. Upon hole doping, the antiferromagnetic order rapidly disappears and the system becomes a superconductor [32-37]. In these compounds the magnetic correlations persist and are still present at optimum doping x_{op} [32, 34, 35].

In low doping regime $x \to 0$, $La_{2-x}Sr_xCuO_4$ is antiferromagntic insulator. When x increases the Neel temperature $T_N(x)$ decreases from its maximum value $T_N(0) = 260$ K and it is suppressed to zero at $x_c = 0.0212$ (Figure **1**). For yttrium compound $YBa_2Cu_3O_{6+x}$, $T_N(x)$ decreases from its maximum value $T_N(0) = 460$ K and it is suppressed at critical doping $x_c = 0.4$ (Figure **2**). The doping dependence of the Neel temperature can be described by the formula: $T_N(x) = T_N(0)\left(1-(x/x_c)^n\right)$ [4, 33].

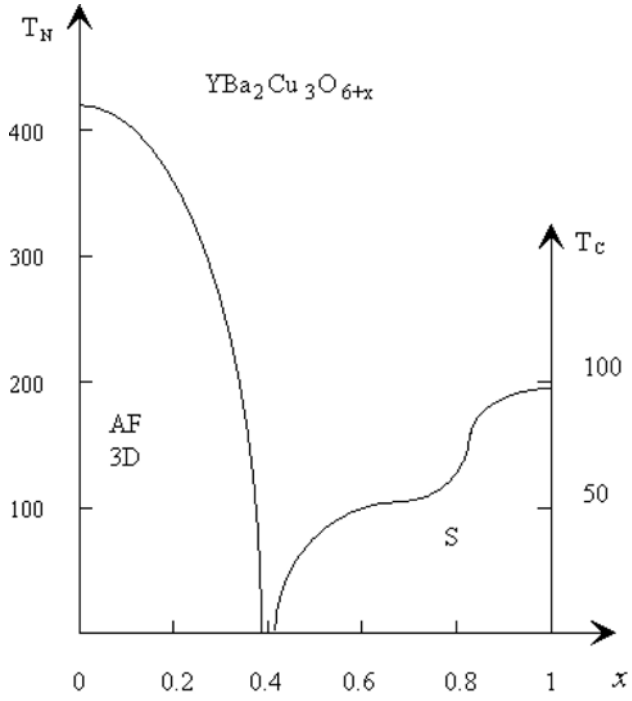

Figure 2: Phase diagram of yttrium compound $YBa_2Cu_3O_{6+x}$ for $0 \le x \le 1$ [35-37].

In $La_{2-x}Sr_xCuO_4$, the occurrence of superconductivity is obtained only after the complete destruction of the three-dimensional AF order. The magnetic correlation length $\xi_m(x)$ decreases with doping and is about equal to the average spacing between the doped holes. The magnetic correlation length $\xi_m(x)$ which is about 1 nm persists in high-T_c. This means that the carriers move against the background of the localized spin lattice. In conventional superconductors, there is no localized spin. This observation leads to assume the positive involvement of some magnetic interaction in the mechanism of high-T_c superconductivity [34].

The yttrium compound $YBa_2Cu_3O_{6+x}$ is an antiferromagnetic in its tetragonal phase at small x, and becomes a superconducting metal in the large x orthorhombic phase. The AF ordering in the tetragonal phase is dominated by localized Cu moments in CuO_2 planes. The Cu moments within the CuO_2 planes order antiferromagnetically because of nearest neighbor super-exchange interaction and the planes couple together antiferromagnetically along the *c* axis. The magnetic order is not destroyed by mobile holes until the tetragonal-orthorhombic phase boundary is reached [35].

In all the high-T_c cuprate superconductors the AF phase is destabilized by the reduction of the electron number in the CuO_2 planes. But in $YBa_2Cu_3O_{6+x}$, this phenomenon occurs in a specific way, with the appearance of the CuO chains distorting the tetragonal lattice to an orthorhombic one, and leading to a strong and immediate reduction of the antiferromagnetic susceptibility $\chi_0(\mathbf{q})$, which no longer diverges, even if the Fermi level ε_F coincides with one of the two singularities [36].

In general, for the high-T_c oxide superconductors there is non-coexistence between superconductivity (S) and three-dimensional (3D) antiferromagnetism, but experimental results show that there is a coexistence between S and 2D AF characterized by a short magnetic correlation length decreasing with *x.* For lanthanum compound $La_{2-x}Sr_xCuO_4$ and bismuth compounds, it has been shown that $T_c(x)$ and $T_N(x)$ disappear together when it becomes metallic for higher x value. This fact suggests that the magnetic excitations can give an attractive interaction between two electrons or holes [37].

The crucial structural element for the unusual superconductivity is the CuO_2 plane. The lanthanum compound $La_{2-x}Sr_xCuO_4$ contains only CuO_2 planes between layers La(Ba)O. There is one CuO_2 plane per unit cell. In yttrium compound, each unit cell contains two CuO_2 planes plus a Cu layer in which oxygen bridges the Cu along just one direction, creating parallel CuO chains [35]. A yttrium plane is between the two CuO_2 planes with also BaO planes above and the so called Cu (I)-O chain planes. The chain CuO causes the *b* parameter to be longer than *a*, so that the structure is orthorhombic. The x oxygen concen-

tration enters only along the *b* axis and not along the *a* axis of these planes. There is a function of *x* a tetragonal-orthorhombic transition with *a* = 3.83 Å and *b* = 3.88 Å; along the direction perpendicular to these planes one can define the *c* axis whose unit cell periodicity is of order 11.7 Å [37]. The good conductivity occurs essentially in CuO_2 planes, while other intermediate planes can be less metallic or even insulating.

3. TYPICAL FEATURES OF HIGH-T_C CUPRATE SUPERCONDUCTORS

We know that the atomic structure of these compounds is very anisotropic, from which also follow electronic anisotropies. The penetration depth λ given by $\lambda_{ab,c}^{-2} \propto n/m_{ab,c}^{*}$ where *n* is the charge carrier density and m^* is the effective mass, is very anisotropic, *i.e* large in *c*-direction than in *ab*-plane: $\lambda_c/\lambda_{ab} \approx 3-10$. This anisotropy of the penetration depth implies anisotropy of the effective mass: $m_c^*/m_{ab}^* \approx 25$. For large anisotropy ratio $\lambda_c/\lambda_{ab} \geq 5$, an effective penetration depth λ_{eff} is independent of the anisotropy ratio and is solely determined by λ_{ab} : $\lambda_{eff} \cong 1.23\lambda_{ab}$ [38, 39]. The values of λ_{ab} and λ_c are deduced from the experimental value of the penetration depth $\lambda_{eff}(0) = 155$ nm and the known anisotropy ratio $\lambda_c/\lambda_{ab} \approx 5$. According to this equation, the following values for the penetration depth at *T* = 0 were calculated for $YBa_2Cu_3O_{6+x}$: $\lambda_{ab}(0) = 130$ nm and $\lambda_c(0) \approx 500-800$ nm. Another interesting problem concerns the anisotropy of the coherence length ξ. For lanthanum compound $La_{2-x}Sr_xCuO_4$, ξ_{ab} is $\approx 20-35$ Å and $\xi_c \approx 4-7$ Å. For yttrium compound $YBa_2Cu_3O_{6+x}$, ξ_{ab} is $\approx 15-16$ Å and $\xi_c \approx 1-3$ Å. We estimate that the ratio ξ_{ab}/ξ_c is about 5 for the cuprate superconductors. Compared to the conventional superconductors, the penetration depth λ is large and the coherence length ξ is much smaller. The small value of ξ_c indicates that between the CuO_2 planes the superconducting order parameter is weaker, a fact related to the superconducting coupling between planes [37]. In addition, it is found that the coherence length ξ_c in the *c*-direction becomes much smaller than the inter-plane distance *l*. It means that the Cooper pairs are concentrated near planes and propagate along the plane. The overlapping of electronic wave functions is very sensitive to small displacements of atoms and thus, may be extremely anisotropic. Electron Bloch wave functions in the normal state of layered metals are rather strongly modulated in the direction *c* perpendicular to conducting *ab* planes [40].

Measurements by tunneling effects of the gap energy $\Delta(0)$ show that the superconducting gap ratio $R = 2\Delta(0)/k_BT_c$ is anisotropic *i.e* large in *ab* planes compared to the *c*-direction [41]. For yttrium compound Y-123, R_{ab} is $\approx 5.6-10$ and $R_c = 3.6$, while for bismuth compounds Bi-2212 and Bi-2223, R_{ab} is $\approx 8-10$ and $R_c = 6$. The electrical resistivity ratio ρ_c/ρ_{ab} is of order 30 for yttrium compound Y-123, of order 200 for lanthanum compound $La_{2-x}Sr_xCuO_4$, even of order 4×10^4 for bismuth compound Bi-2212 [42] and of order 1000 for mercury compound Hg-1223 [43]. This indicates clearly that the good conductivity occurs essentially in the CuO_2 planes.

To study the physical properties of the high-T_c superconductors, it is important to know the Fermi energy, the Fermi velocity, the coupling constant, the effective mass of carriers, etc. These parameters are well known for the conventional superconductors.

It is now well accepted that the origin of superconductivity is found in the CuO_2 planes which are weakly coupled together along the perpendicular axis, so that their electronic structure will be quasi-two dimensional.

All the known high-T_c superconductors have conducting CuO_2 planes separated by insulating layers. Many experimental results [44-47] have identified the presence of saddle points (SP) in the band structure energy. These saddle points produce a van Hove singularity (VHS) in the density of states. In high-T_c Cu oxides, the Fermi velocity is not constant. We know that pure superconductors metal such Al, In, Nb, Pb, Sn and Zn are very well described by the free electron model. For two-dimensional square lattice in this model, the density of states is constant, but for the new superconductors, the presence of the saddle points leads to the singularity in the density of states.

Near the singularity, we consider a two-dimensional electronic spectrum given by [48-50].

$$\varepsilon(k) = \varepsilon_F(1-\gamma) + \frac{\hbar^2}{2m^*}k_xk_y \qquad (1)$$

where ε_F is the Fermi energy and m^* is the effective mass of carriers in CuO_2 plane. The electronic spectrum described by Eq. (1) gives logarithmic singularities in the density of states at $\varepsilon_{VHS} = \varepsilon_F(1-\gamma)$. The parameter γ allows us to control the position of the VHS with respect to the Fermi level, *i.e* $\gamma = (\varepsilon_F - \varepsilon_{VHS})/\varepsilon_F$. The electronic spectrum given by

Eq. (1) has been shown to be in a good agreement with angle-resolved photoemission spectra experiments in high-T_c superconductors and can explain main electronic properties of these new compounds [48]. From Eq. (1), we have the following expression of the density of states near the singularity

$$n_s(\varepsilon) = \frac{dN(\varepsilon)}{d\varepsilon} = \frac{2m^* a^2}{\pi^2\hbar^2} \ln \frac{\pi^2\hbar^2}{4m^* a^2 \left|\varepsilon - \varepsilon_F(1-\gamma)\right|}. \quad (2)$$

Near the band edge, the energy $\varepsilon(k)$ has the form

$$\varepsilon(k) = \frac{\hbar^2 k^2}{2m^*} \quad (3)$$

and the density of states (DOS) is constant in two-dimensional square lattice

$$n_0 = \frac{m^* a^2}{2\pi\hbar^2}. \quad (4)$$

The final density of states $n(\varepsilon)$ takes the form

$$n(\varepsilon) = \frac{2m^* a^2}{\pi^2\hbar^2} \ln \frac{\pi^2\hbar^2}{4m^* a^2 \left|\varepsilon - \varepsilon_F(1-\gamma)\right|} + \frac{m^* a^2}{2\pi\hbar^2}. \quad (5)$$

In the tight-binding model, the energy dispersion is given by $\varepsilon(\mathbf{k}) = -2t\left(\cos k_x a + \cos k_y a\right)$ where t is the transfer integral. The Fermi surface is a perfect square and near the singularity, the density of states is $n(\varepsilon) = (1/2D)\ln(D/\varepsilon)$ where $D = \pi^2 t$ [51]. Near the band edge the two-dimensional electronic spectrum is developed as $\varepsilon(\mathbf{k}) = t((k_x a)^2 + (k_y a)^2)$ which leads to a constant density of states $n_0 = 1/4\pi t$. Another work [52] shows that the density of states $n(\varepsilon)$ derived from a tight-binding model on a two dimensional square lattice contain a logarithmic term plus a constant one. This DOS is given by: $n(\varepsilon) = n_1 \ln(D/\varepsilon) + n_0$, where $n_1 = 1/2\pi^2 t$, $D = 4t$ and $n_0 = (1/2\pi^2 t)\ln 4$. If we take into account the second neighbor interaction *t'*, the singularity is displaced towards lower energy and it occurs for ε = - 4*t'*. In this work, the authors have shown that the additional constant term in $n(\varepsilon)$ enhances the isotope coefficient α. We can write the general density of states as

$$n(\varepsilon) = n_1 \ln \frac{D}{\left|\varepsilon - \varepsilon_F(1-\gamma)\right|} + n_0 \quad (6)$$

where $n_1 = 1/2D$ and $D = \pi^2\hbar^2/4m^* a^2$. For $\gamma = 0$, the Fermi level coincides with the singularity. When the parameter γ increases from 0 to 0.6, the singularity is shifted to lower energy (Figure **3**). With this form of the density of states (γ = 0), we have established analytical expressions of the superconducting gap ratio *R* [53], the critical temperature T_c and the isotope coefficient α [54, 55].

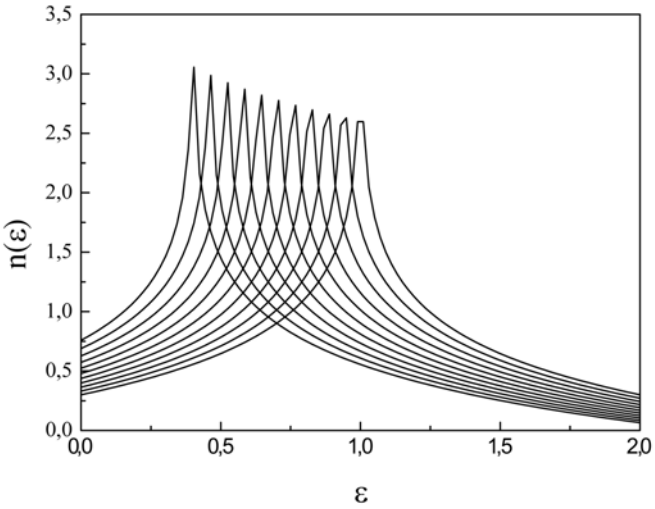

Figure 3: Variation of the density of states $n(\varepsilon)$ with the energy ε for different values of the parameter γ ($\gamma = (\varepsilon_F - \varepsilon_{VHS})/\varepsilon_F$) *i.e.*, γ = 0, 0.06, 0.12, 0.18, 0.24, 0.30, 0.36, 0.42, 0.48, 0.54, 0.60, with $D = \varepsilon_F = 1$ eV, $n_1 = 0.5$ states/eV and $n_0 = 0.3$ states/eV.

For a half-filling system, the Fermi level is just on the singularity $\varepsilon_F = \varepsilon_{VHS}$. We know for half filling, the high-T_c superconductors are antiferromagnetic insulators. The Fermi level is at the VHS for a doping level corresponding to 20 % of holes in each CuO_2 plane or 40 % filling of the Brillouin zone (BZ) [56]. This can be achieved by taking into account the interaction between the second nearest neighbors and the effect of the orthorhombic distortion [57]. The introduction of this orthorhombic distortion increases the value of the superconducting gap ratio *R*, and with decreasing the second neighbor hopping, *R* decreases [58]. The variation of *R* suggests that the Fermi level is shifted from the singularity. We shall mention that this model for the density of states of a two-dimensional system is unstable at half-filling in view of nesting effect [59]. We believe that instability is due to the magnetic excitations or thermodynamic fluctuations. When the Fermi level ε_F coincides with the singularity, a band Jahn-Teller effect is expected, which leads to a structural phase transition from the tetragonal phase to an orthorhombic one [60]. The unique van Hove singularity of the tetragonal phase is splitted into two singularities with the Fermi level lying between them, in a region where

the density of states is low. The low temperature tetragonal (LTT) phase behaves like a static JT phase, in which the tilting of the CuO_6 splits the VHS degeneracy [4, 61, 62] and simultaneously destroys superconductivity [63]. In a static low temperature orthorhombic (LTO) distortion, the octahedra tilt in such a way as to preserve the VHS degeneracy [4, 63]. It has been shown that low temperature tetragonal (LTT) and high temperature tetragonal (HTT) phases can be interpreted as dynamic Jahn-Teller (JT) phases [4, 63, 64].

The Jahn-Teller (JT) effect was initially developed for molecules and applied to isolated impurities in solids. This effect has been already considered as responsible for the high critical temperature in high-T_c superconductors [65-71]. Theories and models have been proposed, in dynamic or static JT form, to explain the fundamental properties of the cuprates [72-75].

The VHS-JT model predicts a competition between structural instability and superconductivity. The role of the singularity in the mechanism of high-T_c superconductivity and the stability of the system are not yet established but we want to stress that this model has already explained a certain number of experimental facts, *i.e* high-T_c [60, 76-78], small isotope effect [78, 79], thermal conductivity [50], linear resistivity and thermopower [49]. We focus on the role of the van Hove singularity that will be present in stable situations. At optimum doping the VHS is close to the Fermi level ε_F in all the cuprate superconductors. The separation $\varepsilon_F - \varepsilon_{VHS} = \gamma\varepsilon_F$ which is identified to the pseudogag Δ_{pg}, is suppressed to zero at optimum doping x_{op} ($\gamma = 0$). This pseudogap $\Delta_{pg} = \varepsilon_F - \varepsilon_{VHS} = \gamma\varepsilon_F$ increases with underdoping, while the superconducting gap Δ_{sg} decreases. For lanthanum compound $La_{2-x}Sr_xCuO_4$, Δ_{pg} is about 220 meV for x = 0, while the pseudogap transition temperature T^* is estimated at 1050 K and $R = 2\Delta_{pg}/k_BT^* = 4.9$. For yttrium compound $YBa_2Cu_3O_{6+x}$, Δ_{sg} is about 19 meV, T^* = 120 K and the ratio $R = 2\Delta_{pg}/k_BT^* = 3.7$ [4]. For bismuth compound Bi-2212, the magnitude of the pseudogap is $\approx 10-20$ meV in low doping regime ($x \le 0.17$). It decreases with doping and disappears at optimum doping x_{op} [80].

The SG and the pseudogap PG are anisotropic. They have maximum values along [100] and [010] directions and have minimum values along [110] direction. Many studies have shown that Δ_{sg} has *d*-wave symmetry and Δ_{pg} has a similar anisotropy where $\Delta_{sg}(\mathbf{k})$ can be expressed as $\Delta_{sg}(\mathbf{k}) = \Delta_{sg}\cos(2\theta)$ and $\Delta_{pg}(\mathbf{k}) = \Delta_{pg}|\cos(2\theta)|$ [81-84]. It believed that the order parameter in cuprate superconductors has purely *d*-wave symmetry [85, 86], but there are a wide variety of experimental data that support *s* or even more complicated types of symmetries (*d*+*s*, *d*+*is*, etc.) [87]. A more reasonable explanation is that the gap has a substantial anisotropy, while still retaining the full point-group symmetry of the crystal, and it also remains nodeless [88].

4. SUPERCONDUCTING PROPERTIES

4.1. Average of the Fermi Velocity

In the conventional superconductors, the Fermi velocity is constant, but for the cuprate superconductors, the Fermi velocity varies from zero to its maximum $v_F^{\max} = \sqrt{2}\pi\hbar/2m^*a$. The maximum of the Fermi velocity $v_F^{\max}$ decreases with the effective mass m^*. From this expression, $v_F^{\max}$ is in the range (1.072 – 3.218)10^7 cm.s^{-1} when m^* is between $2m_0$ and $6m_0$ (m_0 is the free electron mass). The small value of v_F leads to small value of the coherence length. For lanthanum compound $La_{2-x}Sr_xCuO_4$, ξ_0 is estimated between 20 Å and 35 Å. With experimental values of the superconducting gap ratio *R* and the superconducting transition temperature T_c, and BCS formula of the coherence length ξ_0, we obtain the Fermi velocity v_F in the range (1 – 1.859)10^7 cm.s^{-1}. It is interesting to calculate the coherence length with the average of the Fermi velocity $< v_F >$. This average of v_F is given by

$$\hbar < v_F >= \frac{\hbar \int v_F n(k) dk}{\int n(k) dk} \tag{7}$$

where $n(k)$ is the density of states and v_F is the Fermi velocity given by

$$v_F = \frac{1}{\hbar}\frac{d\varepsilon}{dk_\perp}. \tag{8}$$

Introducing Eq. (8) in Eq. (7), we obtain

$$\hbar < v_F >= \frac{a^2}{4\pi^2}\frac{\int_{-\Delta}^{+\Delta} d\varepsilon \int dk}{\int_{-\Delta}^{+\Delta} n(\varepsilon) d\varepsilon}. \tag{9}$$

Finally, we obtain

$$< v_F >= \frac{\sqrt{2}a2D}{\pi\hbar}\frac{1}{\left[1+\frac{n_0}{n_1}+\ln\frac{D}{\Delta}\right]}. \quad (10)$$

The average of the Fermi velocity $< v_F >$ depends on the ratios n_0/n_1 and $\Delta(0)/D$. When $D=16t$, $n_1=1/2\pi^2 t$ and $n_0=0$, we obtain the Bok-Force formula [89]. With Eq. (10), we obtain small values of the Fermi velocity. Our calculation shows that the average value of v_F is in the range (2 - 8)10^6 cm.s^{-1}. These values are smaller than those obtained from the maximum of the Fermi velocity. In conventional metal, the Fermi velocity is in the range (1 - 2)10^8 cm.s^{-1}. The small value of the average of the Fermi velocity leads to small values of the coherence length ξ_0, although the higher T_c also contributes to the decrease in ξ_0.

4.2. Properties of the Coherence Length

In the BCS theory, the coherence length is given by [90]

$$\xi_0 = \frac{\hbar < v_F >}{\pi\Delta(0)}. \quad (11)$$

Introducing Eq. (10) in Eq. (11), we obtain

$$\xi_0 = \frac{2\sqrt{2}}{\pi^2}\frac{aD}{\Delta(0)}\frac{1}{\left[1+\frac{n_0}{n_1}+\ln\frac{D}{\Delta(0)}\right]}. \quad (12)$$

This formula shows that the coherence length depends on the ratios n_0/n_1 and $\Delta(0)/D=\Delta(0)/\varepsilon_F$. The coherence length decreases when the ratio $\Delta(0)/D$ increases: for example when this ratio increases from 0.005 to 0.03, the ratio ξ_0/a decreases from 9.16 to 2.12 for $n_0/n_1=0$ (Figure **4**). In this case if we chose a = 4 Å the coherence length ξ_0 decreases from 36.64 Å to 8.24 Å. This ratio estimates what fraction of the carriers which are directly involved in the pairing. A large gap energy and small value of the width of singularity ($D=\varepsilon_F$) contribute to the large value of the ratio $\Delta(0)/D$. Our calculation shows that this ratio is large in cuprate superconductors ($\Delta(0)/\varepsilon_F \approx 10^{-2}-10^{-1}$). In conventional superconductors, this ratio is very small ($\Delta(0)/\varepsilon_F \approx 10^{-4}$). The large value of this parameter means that significant fraction of the carriers are paired. This corresponds to a short average distance between paired carriers which further implies a short coherence length.

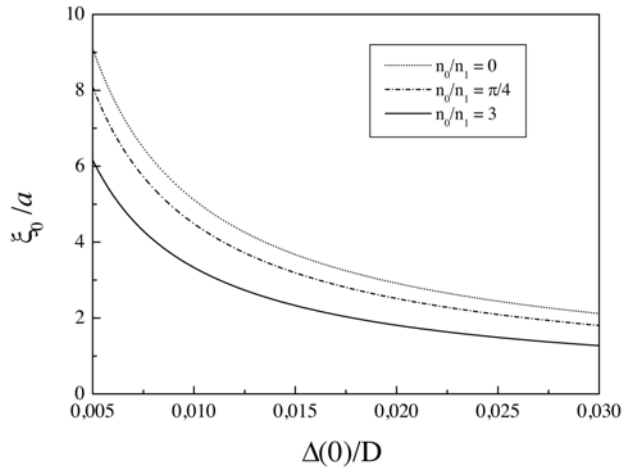

Figure 4: Variation of the coherence length with the ratio $\Delta(0)/D$ for different values of the ratio n_0/n_1.

The possibility of having a large value of $\Delta(0)/\varepsilon_F$ and short coherence length is related to the quasi-2D structure of the high-T_c superconductors [91]. The large value of this parameter describes other properties such a scale of the critical region near T_c. In addition, we mention that the parameter $\left(\Delta(0)/\varepsilon_F\right)^2$ describes the shift in the dielectric function due to superconducting transition. This shift is negligibly small in conventional superconductors, but it is noticeable in high-T_c oxide superconductors [91].

The expression of the gap energy is given by [79]

$$\Delta(0) = 2D\exp\left\{\frac{n_0}{n_1}-\left[\frac{2}{n_1V_p}+\left(\frac{n_0}{n_1}+\ln\frac{D}{\hbar\omega_0}\right)^2-p\right]^{\frac{1}{2}}\right\} \quad (13)$$

where p = 1.64. From this expression, we have

$$\frac{\Delta(0)}{2D} = \exp\left\{\frac{n_0}{n_1}-\left[\frac{2}{n_1V_p}+\left(\frac{n_0}{n_1}+\ln\frac{D}{\hbar\omega_0}\right)^2-p\right]^{\frac{1}{2}}\right\} \quad (14)$$

and

$$\ln\frac{\Delta(0)}{D} = -\ln 2-\frac{n_0}{n_1}+\left[\frac{2}{n_1V_p}+\left(\frac{n_0}{n_1}+\ln\frac{D}{\hbar\omega_0}\right)^2\right]^{\frac{1}{2}}. \quad (15)$$

Introducing Eqs. (14) and (15) in Eq. (12), we obtain

$$\xi_0 = \frac{a\sqrt{2}}{\pi^2 e^{n_0/n_1}}\frac{\exp\left[\frac{2}{n_1V_p}+\left(\frac{n_0}{n_1}+\ln\frac{D}{\hbar\omega_0}\right)^2-p\right]^{\frac{1}{2}}}{q+\left[\frac{2}{n_1V_p}+\left(\frac{n_0}{n_1}+\ln\frac{D}{\hbar\omega_0}\right)^2-p\right]^{\frac{1}{2}}} \quad (16)$$

where q = 0.3068. This expression depends on the phonon interaction V_p, on the width of singularity D, on the vibrational energy $\hbar\omega_0$ and on the ratio n_0/n_1. Numerical calculation shows that ξ_0 decreases when the effective mass of carriers m^* increases. The coherence length decreases with the coupling constant $\lambda_p = n_1 V_p$. Figure (**5**) shows that when the coupling constant λ_p increases from 0.06 to 0.173, the coherence length decreases from 44.48 Å to 8 Å for $n_0 = 0$ and from 24.8 Å to 5.15 Å for $n_0 = n_1$ ($D = 0.645$ eV, $\hbar\omega_0 = 0.045$ eV). In weak coupling limit (λ_p = 0.06 – 0.173), we obtain small values of coherence length ξ_0. These values are in a good agreement with experimental results.

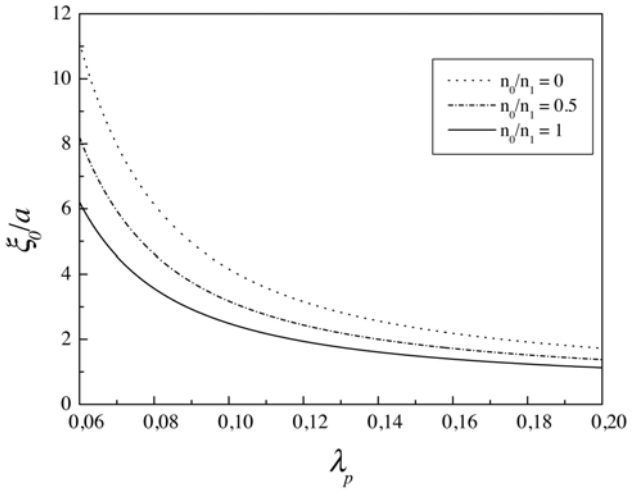

Figure 5: Variation of the coherence length ξ_0 with the coupling constant λ_p for different values of the ratio n_0/n_1 ($D = 0.645$ eV , $\hbar\omega_0 = 0.045$ eV).

4.3. Properties of the Isotope Effect

One of the most interesting properties of the cuprate superconductors is the variation of the isotope coefficient with the hole concentration x. When the concentration increases, the superconducting transition $T_c(x)$ increases and reaches its maximum at optimum doping x_{op}, while the isotope coefficient α decreases and reaches its minimum at x_{op}. In low doping regime, the isotope coefficient is large, but it is almost negligible in high doping regime. The isotope coefficient α which is maximum at the border to the antiferromagnetic states, decreases with doping and takes small values at optimum doping. The fact that the isotope effect is not negligible reveals the role played phonons. The small value of α at high doping regime leads to suggestion that the attractive interaction between holes or electrons might be related to another mechanism with a possible phononic contribution.

It is well established that magnetic correlations play a crucial role in the superconducting state [92, 93]. Experimental results show that there is coexistence between the superconducting state and two-dimensional AF of the CuO_2 planes with a short magnetic correlation length which decreases with x. For lanthanum $La_{2-x}Sr_xCuO_4$ and 2212 bismuth compound, it has been shown that the superconducting transition temperature $T_c(x)$ and the Neel temperature $T_N(x)$ disappear together when it becomes metallic for higher x values. This suggests that the attractive interaction between holes or electrons is related to the magnetic excitations. It has been shown that high-temperature superconductivity in cuprates can be understood in terms of an interacting hole-spin model with super-exchange and Kondo-type exchange interactions [31]. In this model, at high temperature holes form Cooper pairs via singlet-triplet excitation in localized 3d spin system.

We consider this interaction – V_m (V_m >0) constant from –W/2 to +W/2 where W is the bandwidth (W = 2D). This interaction has the form [31]

$$V_m = \frac{K^2}{J} = \frac{K^2}{J_0}\exp\left(\frac{1}{2d^2}\frac{\hbar}{2M\omega_0}\right) \tag{17}$$

where d is a characteristic length for the overlap of wave functions, M is the mass of an oxygen or copper ion and $\hbar\omega_0$ is the $\mathrm{Cu-O}$ vibrational energy. In the weak coupling approach, the superconducting transition temperature T_c is determined by the gap equation

$$\frac{1}{V_m} = \int_0^D \frac{n(\varepsilon)}{\varepsilon}\tanh\left(\frac{\varepsilon}{2k_B T_c}\right). \tag{18}$$

From Eq. (6) and Eq. (18), we obtain the following expression of T_c

$$k_B T_c = 1.13D\exp\left\{\frac{n_0}{n_1} - \left[\frac{2}{n_1 V_m} + \left(\frac{n_0}{n_1}\right)^2 - p\right]^{\frac{1}{2}}\right\}. \tag{19}$$

If we neglect the singularity ($n_1 \to 0$) and we take $D = J$, we obtain the Kuruhara formula. The superconducting transition temperature T_c increases with the coupling constant $\lambda_m = n_1 V_m$ (Figure **6**): for example T_c increases from 15.15 K to 90.82 when λ_m varies from 0.03 to 0.050 ($D = 0.645$ eV and $n_0/n_1 = 2$). T_c increases with the ratio n_0/n_1: for example, when the ratio n_0/n_1 varies from 1 to 2, T_c increases from 19.36 K to 44 K for λ_m = 0.04 and from 42.21 K to 90.82 K for λ_m = 0.05.

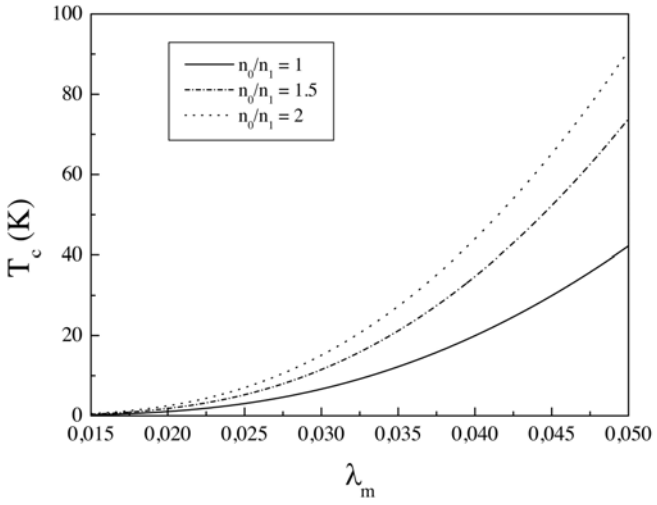

Figure 6: Variation of the superconducting transition temperature T_c with the coupling constant $\lambda_m = n_1 V_m$ for different values of the ratio n_0/n_1 ($D = 0.645$ eV).

To study the isotope effect, we consider the variation of the superconducting transition temperature T_c when varying ω_0. We know that ω_0 varies like $M^{-1/2}$ where M is the nuclear mass. The isotope coefficient defined by the expression $T_c \propto M^{-1/2}$ can be calculated from the following expression

$$\alpha = -\frac{\partial \ln T_c}{\partial \ln M} = \frac{1}{2}\frac{\partial \ln T_c}{\partial \ln \omega_0}. \tag{20}$$

To determine the coefficient α, we differentiate Eq. (19) with respect to ω_0. We finally obtain the following expression of the total isotope effect.

$$\alpha = \alpha_O + \alpha_{Cu} = \frac{1}{4n_1 V_m}\frac{1}{\left[\frac{2}{n_1 V_m} + \left(\frac{n_0}{n_1}\right)^2 - p\right]^{\frac{1}{2}}}\left(\frac{1}{2d^2}\frac{\hbar}{\omega_0}\right)\left(\frac{1}{M_O} + \frac{1}{M_{Cu}}\right) \tag{21}$$

We can write this expression as the simple form

$$\alpha = \alpha_O + \alpha_{Cu} = \frac{1}{4\lambda_m}\frac{\left(\beta_O + \beta_{Cu}\right)}{\left[\frac{2}{\lambda_m} + \left(\frac{n_0}{n_1}\right)^2 - p\right]^{\frac{1}{2}}} \tag{22}$$

where $\lambda_m = n_1 V_m$, $\beta_O = \hbar/2d^2\omega_0 M_O$ and $\beta_{Cu} = \hbar/2d^2\omega_0 M_{Cu}$. We can also write this expression as

$$\alpha = \alpha_O + \alpha_{Cu} = \frac{1}{4\lambda_m}\frac{\left(\beta_O + \beta_{Cu}\right)}{\left[\frac{n_0}{n_1} + \ln\frac{1.13D}{k_B T_c}\right]^{\frac{1}{2}}}. \tag{23}$$

For $d = 0.5$ Å, when $\hbar\omega_0$ is between 0.020 eV and 0.085 eV, the parameter β_0 is between 2.616 × 10^{-2} and 0.6155 × 10^{-2} and the parameter $\beta_T = \beta_O + \beta_{Cu}$ is between 3.27 × 10^{-2} and 0.77 × 10^{-2}.

Equation (22) shows that the total isotope coefficient α decreases with the coupling constant λ_m. When the coupling constant λ_m increases, the superconducting temperature transition T_c increases, while the total isotope coefficient decreases. When λ_m varies from 0.03 to 0.05, the oxygen isotope coefficient α_0 decreases from 0.0269 to 0.021 for $\beta_O = 2.616\times10^{-2}$ and from 0.015 to 0.012 for $\beta_O = 1.500\times10^{-2}$. The parameter n_0/n_1 has not a large effect on α_o. Our calculation shows that when T_c increases α_o decreases. These values are in a good agreement with experimental values of isotope coefficient in yttrium and bismuth compounds. For lanthanum compound $La_{2-x}Sr_xCuO_4$, we obtain small values of α_o compared to experimental values (0.06 - 0.15). In a previous work, we have established an expression of the isotope coefficient depending simultaneously on phonons and magnetic interactions [54]. In this work, we have shown that when T_c increases, the isotope coefficient α_o decreases from its maximum ≈ 0.38 - 0.40 to its minimum 0-0.05.

For the electron-doped superconductors ($Nd_{2-x}Ce_xCuO_4$), the oxygen isotope coefficient is very small ($\alpha_O < 0.05$ with $T_c^{\max} \approx 24$ K). These compounds are very well described by this model.

Figure (**6**) shows that when the coupling constant λ_m increases from 0.02 to 0.05, the superconducting transition temperature T_c increases from 2.5 K to 90.89 K ($D = 0.645$ eV, n_0/n_1 = 2). We remark that even weak interaction can produce a large effect on T_c: for example when λ_m varies from 0.048 to 0.056 ($\Delta\lambda_m$ = 0.008), T_c varies from 80.14 K to 114.47 K (ΔT_c = 34.33 K). In this case, the isotope coefficient $\alpha = \alpha_O + \alpha_{Cu}$ decreases from 0.13 to 0.025 for $\beta_T = 3.270\times10^{-2}$ ($\hbar\omega_0 = 0.020$ eV), and from 0.030 to 0.006 for $\beta_T = 0.770\times10^{-2}$ ($\hbar\omega_0 = 0.085$ eV), (Figure **7**). We expect that vibrations of copper and oxygen ions could be important in giving high-T_c.

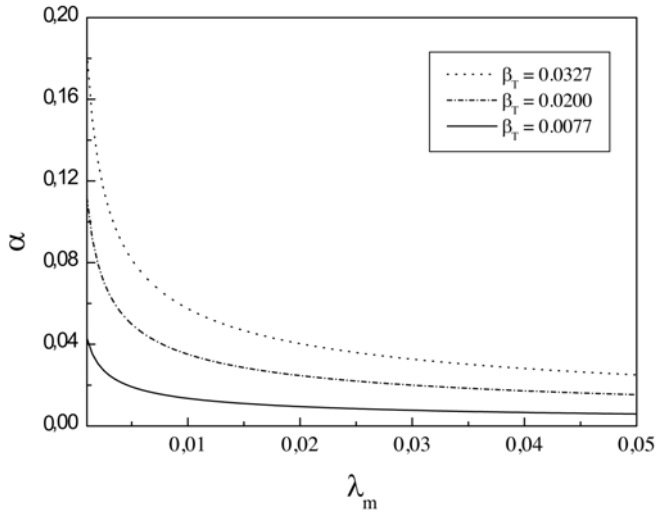

Figure 7: Variation of the isotope coefficient $\alpha = \alpha_O + \alpha_{Cu}$ with the coupling constant $\lambda_m = n_1 V_m$ for different values of the parameter $\beta_T = \beta_O + \beta_{Cu}$ ($n_0/n_1 = 2$).

Other numerical calculation shows that when the magnetic coupling constant varies from 0.04 to 0.08, T_c increases from 19.35 K to 154.87 K, while the coefficient α decreases from 0.0446 to 0.0224 ($D = 0.625$ eV and $n_0/n_1 = 1$). The yttrium compound $YBa_2Cu_3O_{6+x}$ and bismuth compounds Bi-2212 and Bi-2223 are very well described by Eq. (22). For thallium and mercury compounds which the isotope effect is unknown, we believe that this effect exists, but we cannot detect it experimentally. For lanthanum compound $La_{2-x}Sr_xCuO_4$, the total isotope coefficient α obtained from Eq. (22) is very smaller than the experimental values (0.06 – 0.15). We conclude that both phonon and magnetic interaction contribute to the isotope effect in $La_{2-x}Sr_xCuO_4$.

At low temperature the attractive interaction is due essentially to the phonons V_p and the isotope coefficient α_p is in the range 0.38 – 0.40. When the temperature increases, the interaction due to the phonons V_p decreases while the interaction due to the magnetic excitations V_m increases [54]. At high temperature the interaction is due essentially to the magnetic excitations and the isotope coefficient α_m is in the range 0.006 – 0.05. When the temperature increases, this coefficient decreases from its maximum value (0.38 - 0.40) to its minimum value (0.006 – 0.05). These results of calculation are in qualitative agreement with experimental data.

In the van Hove scenario, both in weak and strong coupling cases [94], the values of the isotope coefficient ($\alpha \approx 0.15 - 0.25$) are greater than experimental results ($\alpha \approx 0.02 - 0.06$).

In Jahn-Teller model [68], one obtains both positive and negative value of the isotope coefficient α. The values of α are in a good agreement with experimental data of the lanthanum and yttrium compounds. This model explains some negative values observed in yttrium and bismuth compounds [21].

In the van Hove scenario with a weak coupling model of charge density waves (CDWs) [95], the isotope coefficient can become very small in comparison with $0.5 > \alpha_{CDW} > 0.39$ for Balseiro–Falicov model [96] but these values are still larger than the experimental data. On the other hand, Yndurain has studied the variation of the isotope coefficient with hole concentration x, considering spin density waves (SDWs) in two-dimensional systems [97]. In this model, it has found that the isotope cofficient α varies abruptly near the hole concentration where the superconducting transition temperature is maximum. This coefficient decreases with x and reach its minimum $\approx 0.06 - 0.09$ at optimum doping x_{0p}, corresponding to a maximum in T_c. This behavior of α is related to the coexistence of SDW and superconductivity [97]. For yttrium compound $YBa_2Cu_3O_{6+x}$, it has shown that the isotope coefficient α decreases with the superconducting transition temperature T_c. In this model, the results of the calculation are in qualitative agreement with experimental data.

4.4. Properties of the Superconducting Gap Ratio $R = 2\Delta(0)/k_BT_c$

The high-T_c superconductors are characterized by a large value of the superconducting gap ratio $R = 2\Delta(0)/k_BT_c$. This ratio has an ordinary magnitude 3.53 in conventional superconductors, but it is much larger, being 5 - 13 for the new superconductors. The large superconducting gap ratio is expected to be associated with strong anisotropy [88]. The large value of this parameter is still not understood. Various approaches based on electronic as well as phonon-based interaction, sometimes for isotropic *s*-wave and other times for *d*-wave pairing, have been proposed to explain the large value of R [95, 98-105] but the maximum values of this parameter are still much lower than the experimental results.

In Jahn-Teller model, one obtains large value of the superconducting gap ratio *R*: $3.53 \le R \le 7$ [68]. These values are greater than the classical BCS value 3.53, but are still smaller than experimental results ($\approx 7 - 13$) of the hole-doped cuprates.

In two-dimensional charge density waves (CDWs), the superconducting gap ratio R varies very little from the BCS value 3.53. The maximum value of this ratio is $R_{CDW} = 2\Delta(0)/k_BT_{c,CDW} = 3.74$ [95]. Large values of

R ($R = 2\Delta(0)/k_B T_c \approx 5-8$) can be obtained in CDW model [106]. These theoretical values are still smaller than experimental results ($\approx 7-13$).

In the van Hove scenario, with competition between conventional BCS superconductivity and spin density waves (SDWs) [97], the gap energy is obtained by using Eq. (6) with $n_0 = 0$ and the superconducting gap ratio is in the range $\approx 3.53-3.68$ in s-wave and $\approx 4-5$ in d-wave symmetry.

At low temperature the attractive interaction is due essentially to the phonons and the superconducting gap R varies very little from the BCS value ($R = 3.53-3.68$) in *s*-wave and from 4 to 5 in *d*-wave symmetry. This is a very small variation between R_d and R_s ($R_d - R_s \approx 1-1.47$). Both in *s*-wave and *d*-wave symmetry, the theoretical values of R are still smaller than experimental values.

At high temperature, the attractive interaction is related to the magnetic excitations [54]. Equations (13) and (19) lead to the following expression of the superconducting gap ratio R

$$R = 3.53\exp\left\{\left[\frac{2}{n_1 V_m} + \left(\frac{n_0}{n_1}\right)^2 - p\right]^{\frac{1}{2}} - \left[\frac{2}{n_1 V_p} + \left(\frac{n_0}{n_1} + \ln\frac{D}{\hbar\omega_0}\right)^2 - p\right]^{\frac{1}{2}}\right\} \quad (24)$$

The parameter R has the ordinary BCS value ≈ 3.53 when

$$\lambda_p = \frac{\lambda_m}{1 - \lambda_m\left[\frac{n_0}{n_1}\ln\frac{D}{k_B\theta_0} + \frac{1}{2}\left(\ln\frac{D}{k_B\theta_0}\right)^2 - 0.16\right]}. \quad (25)$$

To have this ratio greater than the BCS value, the coupling constant λ_p must be greater than the coupling constant related to the magnetic excitations λ_m. Figure (**8**) shows that When the coupling constant λ_p increases from 0.079 to 0.120, the superconducting gap ratio *R* increases from the 5.99 to 13.18 for $\lambda_m = 0.048$ corresponding to T_c = 88.14 K, and increases from 3.53 to 9 for $\lambda_m = 0.054$ corresponding to T_c = 114.47 K (D = 0.645 eV, n_0/n_1 = 2 and $\hbar\omega_0 = 0.045$ eV). We remark that even weak interaction can produce a large effect on the superconducting gap ratio *R*: for example, when λ_m varies from 0.048 to 0.054 ($\Delta\lambda_m$ = 0.006), *R* varies from 13.18 to 9 (ΔR = 4.18).

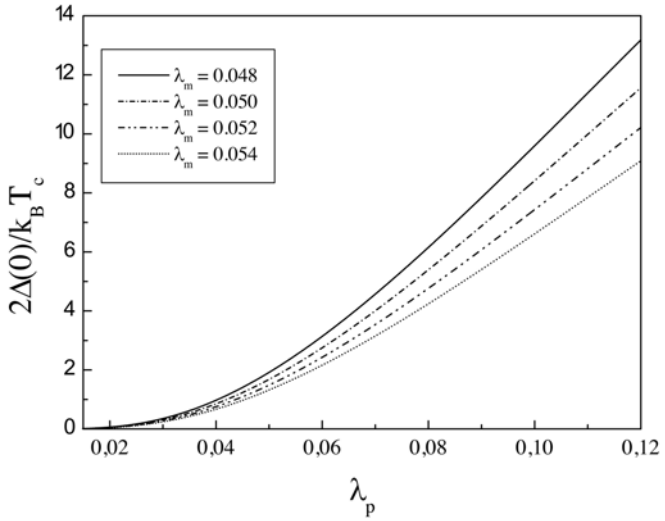

Figure 8: Variation of the superconducting gap ratio R with the coupling constant $\lambda_p = n_1 V_p$ for different values of the coupling constant due the magnetic excitations λ_m, with $D = 0.645$ eV, $\hbar\omega_0 = 0.065$ eV and n_0/n_1 = 1.

Figure (**9**) shows the variation of the superconducting gap ratio *R* with the coupling constant λ_p. When λ_p varies from 0.0725 to 0.120, *R* increases from the BCS value 3.53 to 9 for $\hbar\omega_0 = 0.045$ eV, and from 5 to 13.69 for $\hbar\omega_0 = 0.085$ eV ($D = 0.645$ eV and $\lambda_m = 0.05$).

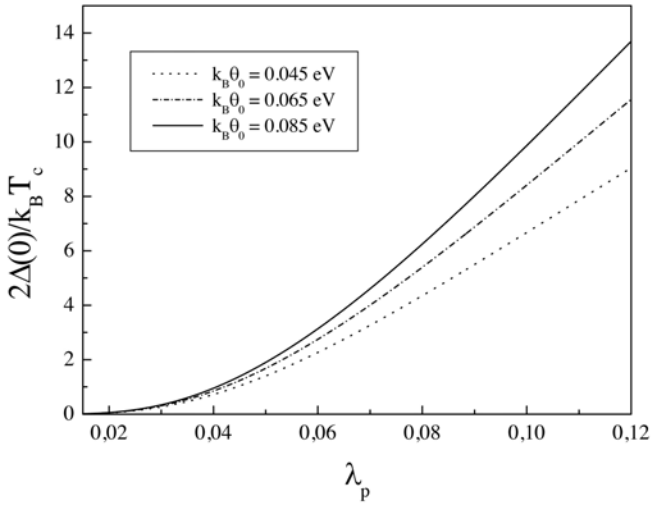

Figure 9: Variation of the superconducting gap ratio with the coupling constant $\lambda_p = n_1 V_p$ for different values of the vibrational energy $\hbar\omega_0$ with $D = 0.645$ eV, $n_0/n_1 = 1$ and $\lambda_m = 0.05$.

At low temperature, our calculation shows that the superconducting gap ratio *R* is equal to the BCS value 3.53. This parameter is exactly evaluated numerically and it was found that it deviates very little from the BCS value 3.53. When the Fermi level lies close to the van Hove singularity, the value of R is in the range 3.53 –

3.68 in *s*-wave, but in *d*-wave symmetry, the value of R is still significantly enhanced from the BCS value 3.53. The maximum value of R is ≈ 5 when $\omega_0/T_c \to 0$ and the minimum value is predicted to be 4.3 in the limit $\omega_0/T_c \to \infty$ [105]. The maximum value of *R* in *d*-wave symmetry is still much lower than experimental values.

In order to have high-T_c (38 –135 K), experimental values of the gap energy and large values of the superconducting gap ratio, the coupling constant due to the magnetic excitations λ_m must be smaller than that corresponding to the phonons λ_p.

Numerical calculations show that when λ_m is in the range 0.020-0.06 and λ_p is in the range 0.03-0.12, the superconducting gap ratio R varies from the BCS value 3.53 to 13. These values are in qualitative agreement with experimental results.

5. CONCLUSION AND DISCUSSION

The high-T_c cuprate superconductors are antiferromagnetic insulators at $x = 0$. Upon hole doping, the AF order rapidly disappears and the system becomes a superconductor. In these compounds the magnetic correlations persist and are still present at optimum doping x_{op}. The occurrence of superconductivity is obtained only after the complete destruction of the three-dimensional AF order. The magnetic correlation length $\xi_m(x)$ decreases with doping and is about equal to the average spacing between the doped holes. The magnetic correlation length $\xi_m(x)$ which is about 1 nm persists in high-T_c. In another words there is coexistence between superconductivity and two-dimensional AF. The superconducting transition temperature $T_c(x)$ and the Neel temperature $T_N(x)$ disappear together for higher *x* values. This fact tends to show that this 2D AF favors superconductivity because the corresponding magnetic excitations can give an attractive interaction between two electrons or holes.

The origin of superconductivity is now found to be in CuO_2 planes which are weakly coupled together to the *c* direction, so that their electronic properties are almost two dimensional. The quasi-2D structure of cuprate superconductors leads naturally to van Hove singularities in the density of states. We expect that these singularities lead to the magnetic excitations. The pseudogap which is identified to the separation $\varepsilon_F - \varepsilon_{VHS} = \gamma\varepsilon_F$, appears at T^*. When the temperature *T* decreases, the PG increases and reaches its maximum at $T > T_c$. From its maximum, $\Delta_{pg}(T)$ decreases when T decreases, and it is suppressed at $T < T_c$. The total gap $\Delta(T) = \sqrt{\Delta_{sg}^2(T) + \Delta_{pg}^2(T)}$ is nearly constant and consistent with experimental results. At low temperature, the total gap becomes a pure SC gap, but at high temperature it is a pure pseudogap ($T_c < T < T^*$), and at intermediate temperatures the gap has two contributions, one form the superconducting gap and the other form the pseudogap. This pseudogap $\Delta_{pg} = \varepsilon_F - \varepsilon_{VHS} = \gamma\varepsilon_F$ decreases with doping *x* and it is suppressed to zero at optimum doping x_{op} ($\gamma = 0$) while the superconducting gap Δ_{sg} increases and reaches its maximum at x_{op}.

In the weak coupling constant ($\lambda_p \approx 0.03 - 0.12$), we obtain simultaneously large value of the gap energy $\Delta(0) = \Delta_{sg}(0)$ and small values of the coherence length ξ_0. The values obtained in this model are in a good agreement with experimental results.

In the Jahn-Teller (JT) limit, the structural distortion splits the degeneracy of two singularities, driving one below and the other above the Fermi level. The strong electron-phonon coupling can be described as a form of band Jahn-Teller effect (JT), with the two symmetry-related van Hove singularities playing the role of degenerate electronic sates. This effect can lead to a phase of short range order (dynamic JT phase), which can lead to the appearance of the pseudopag [63].

In the VHS-JT model, we can obtain simultaneously high T_c, small isotope coefficient and large superconducting gap ratio R. In this model, transport properties, namely resistivity and thermopower are found to be strongly dependent on the variations of the pseudogap [2]. It is interesting to develop the JT model in the van Hove scenario and compare with our results.

In two-dimensional spin density waves (SDWs) model, the separation between the two peaks of the density of states decreases with doping *x* and is proportional to SDW order parameter Δ_{SDW} [97]. This order parameter is large at the superconducting critical temperature. In this model the superconducting gap ratio R varies very little from the BCS value, while the isotope coefficient reaches its minimum, corresponding to a maximum in T_c.

Conventional superconductivity and charge density waves (CDWs) are produced by strong electron-phonon interaction V_p. On the other hand, spin density waves (SDWs) are originated by a strong electron-electron repulsion V_C which tends to destroy superconductivity. The large value of V_p favors

superconductivity and destroys SDW. For small values of both V_p and V_C both possible broken symmetries destroy each other giving rise to a paramagnetic phase. However, for large values of both V_p and V_C both superconductivity and SDW coexist in a large portion of the phase space [97].

The competition between superconductivity and spin density waves (SDWs) has been discussed by Yndurain F in Ref. [97], while the competition between superconductivity and charge density waves (CDWs) has been analyzed by Balseiro CA and Falicov LM in Ref. [96].

Experimental results show that there is coexistence between charge or spin density waves (CDWs or SDWs) and superconductivity in $La_{2-x}Sr_xCuO_4$ and $YBa_2Cu_3O_{6+x}$ [107-109]. The CDW is strongest with the longest in-plane correlation length near 1/8 doping. On entering the superconducting state the CDW is suppressed [107]. In low doping situation the long range antiferromagnetic order is destroyed to give rise to SDW state accompanied by a CDW state in the system due to doping. For suitable doping the superconductivity appears in the system [110]. The significance of the various forms of CDW and SDW is still not understood. Their detection, characterization and relationship with superconductivity remain open problems.

Theories and models of SDW and CDW have been proposed to explain the fundamental properties of high-T_c cuprate superconductors [95-97, 106, 110]. In these works, it has been shown that the pseudopgap Δ_{pg} can be described by CDW state. These experimental and theoretical works forge a path for studying the relationship between superconductivity and CDW or SDW in various superconductors and other materials.

In low temperature the isotope coefficient is large but at high temperature this coefficient is very small. This suggests that the attractive interaction is due to the phonons at low temperature, but at high temperature it is related to the magnetic excitations. When the superconducting transition temperature T_c increases the isotope coefficient α decreases from its maximum value $\alpha_p \approx 0.38 - 0.40$ to its minimum value $\alpha_m \approx 0.006 - 0.05$.

Numerical calculations show that when λ_m is in the range 0.020-0.06 and λ_p is in the range 0.03-0.12, the superconducting gap ratio R varies from the BCS value to 13.

To summarize, we have developed the Kurihara model and obtained analytical expressions for the isotope coefficient α and the superconducting gap ratio R which have been derived with the van Hove singularity in the weak coupling case. With these expressions, we obtain simultaneously the experimental values of these two parameters. From this study, we conclude that the van Hove singularity and the interaction due to the magnetic excitations could play a fundamental role in the mechanism of superconductivity in high-T_c cuprate superconductors.

The competition between phonons and magnetic excitations, in the van Hove scenario, can provide a basis for understanding the high T_c, large superconducting gap ratio R, short coherence length ξ_0 and small isotope coefficient α, and possibly the origin of high-temperature superconductivity.

Such an approach may reconcile VHS-JT model and all observations leading sometimes to spin density waves (SDWs) and other times to charge density waves (CDWs).

ACKNOWLEDGMENTS

It is a great honor for me to write this paper for the inaugural issue of the International Journal of Advanced Applied Physics Research (IJAAPR). I am very grateful to Markiewicz RS, Brandow B, Apostol M, Bouvier J and Bok J for sending their interesting papers.

REFERENCES

[1] Bednorz JG, Müller KA. Possible high T_c superconductivity in the Ba-La-Cu-O system. Z Phys B. 1986; 64(2): 189-193.

[2] Chaudhuri I, Taraphder A, Ghatak SK. Pseudogap and its influence on normal and superconducting states of cuprates. Physica C. 2001; 353 (1-2): 49-59.

[3] Tallon JL, Bernhard C, Shaked H, Hitterman RL, Jorgensen JD. Generic superconducting phase behavior in high-T_c cuprates: T_c variation with hole concentration in $YBa_2Cu_3O_{7-\delta}$. Phys Rev B. 1995; 51(18): R12911-R12914.

[4] Markiewicz RS. A survey of the van Hove scenario for high-T_c superconductivity with special emphasis on pseudogaps and striped phases. J Phys Chem Solids. 1997; 58(8): 1179-1310.

[5] Markiewicz RS, Sahrakorpi S, Lindroos M, Lin H, Bansil A. One-band tight-binding model parametrization of the high-T_c cuprates including the effect k_z dispersion. Phys Rev B. 2005; 72(5): 054519-054531.

[6] Das T, Markiewicz RS, Bansil A. A competing order scenario of two-gap behavior in hole doped cuprates. arXiv:0711.0480v1 [cond.mat.supr-con] 3 Nov 2007.

[7] Borne AJH, Carbotte JP, Nicol EJ. Signature of pseudogap formation in the density of states of underdoped cuprates. arxiv:1006.3232v1[cond-mat.supr-con] 16 Juin 2010.

[8] Kanigel A, Norman MR, Randeria M, Chatterjee U, Souma S, Kaminski A, *et al*. Evolution of the pseudogap from Fermi

arcs to the nodal liquid. Nature Physics. 2006; 2: 447-451; Kanigel A, Chatterjee U, Randeria M, Norman MR, Souma S, Shi M, *et al*. Protected nodes and the collapse of Fermi arcs in high-T_c cuprate superconductors. Phys Rev Lett. 2007; 99(15**)**: 157001-157004.

[9] Moca CP, Tifrea I, Crisan M. An analytical approach for the pseudogap in the spin fluctuations model. J Supercond Incorp Novel Mag. 2000; 13(3): 411-416.

[10] Dzhumanov S, Ganiev OK, Djumanov SS. Novel isotope effects on the pairing pseudogap in high-T_c cuprates: Evidences for polaronic metal and precursor BCS-like pairing of large polarons. arXiv:1006.2892v1[cond.mat.supr.con] 15 Juin 2010.

[11] Welp U, Kwok WK, Crabtree GW, Vandervoort KG, Liu JZ. Magnetic measurements of the upper critical field of YBa2Cu3$O_{7-\delta}$ single crystals. Phys Rev Lett. 1989; 62(16):1908-1911.

[12] Hao Z, Clem JR, McElfresh MW, Civale L, Malozemoff AP, Holtzberg F. Model for the reversible magnetization of high-κ type-II superconductors: Application to high-T_c superconductors. Phys Rev B. 1991; 43(4): 2844-2852.

[13] Brandstätter G, Sauerzopf FM, Weber HW, Ladenberger F, Schwarzmann E. Upper critical field, penetration depth, and GL parameter of Tl-2223 single crystals. Physica C. 1994; 235-240(3): 1845-1846.

[14] Li Q, Suenaga M, Hikata T, Sato K. Two-dimensional fluctuations in the magnetization of $Bi_2Sr_2Ca_2Cu_3O_{10}$. Phys Rev B. 1992; 46(9): 5857-5860.

[15] Batlogg B, Kourouklis G, Weber W, Cava RJ, Jayaraman A, White AE, *et al*. Nonzero isotope effect in $La_{1.85}Sr_{0.15}CuO_4$. Phys Rev Lett. 1987; 59(8): 912-914.

[16] Batlogg B, Cava RJ, Jayaraman A, van Dover RB, Kourouklis GA, Sunshine S, *et al*. Isotope effect in the high-T_c superconductors $Ba_2YCu_3O_7$ and $Ba_2EuCu_3O_7$. Phys Rev Lett. 1987; 58(22) 2333-2336.

[17] Katayama-Yoshida H, Hirooka T, Oyamada A, Okabe Y, Takahashi T, Sasaki T, *et al*. Oxygen isotope effect in the superconducting Bi-Sr-Ca-Cu-O system. Physica C. 1988; 156(3): 481-484.

[18] Franck JP, Harker S, Brewer JH. Copper, oxygen isotope effects in $La_{2-x}Sr_xCuO_4$. Phys Rev Lett. 1993; 71(2): 283-286.

[19] Crawford MK, Farneth WE, McCarron EM, III, Harlow RL, Moudden AH. Oxygen isotope effect and structural phase transitions in La_2CuO_4-based superconductors. Science. 1990; 250: 1390-1394.

[20] Franck JP, Jung J, Mohamed MAK, Gygax S, Sproule GI. Observation of an oxygen isotope effect in superconducting $(Y_{1-x}Pr_x)Ba_2Cu_3O_{7-\delta}$. Phys Rev B. 1991; 44(10): 5318-5321.

[21] Kulé ML. Importance of the electron-phonon interaction with the forward scattering peak for superconducting pairing in cuprates. J Supercond Novel Magnetism. 2006; 19(3-5): 213-249.

[22] Ekino T, Doukan T, Fujii H, Nakamura F, Sakita S, Kodama M, *et al*. Superconducting energy gap of $La_{1.85}Sr_{0.15}CuO_4$ single crystals from break-junction tunneling. Physica C. 1996; 263(1-4): 249-252.

[23] Yu G, Li Y, Motoyama EM, Greven M. A universal relationship between magnetic resonance and superconducting gap in unconventional superconductors. Nature Phys. 2009; 5: 873-875.

[24] Wei JYT, Tsuei CC, van Bentum PJM, Xiong Q, Chu CW, Wu MK. Quasiparticle tunneling spectra of the high-T_c mercury cuprates: Implications of the d-wave two-dimensional van Hove scenario. Phys Rev B. 1998; 57(6): 3650-3662.

[25] Lee WS, Vishik IM, Tanaka K, Lu DH, Sasagawa T, Nagaosa N, *et al*. Abrupt onset of a second energy gap at the superconducting transition of underdoped Bi2212. Nature (London). 2007; 450: 81-84.

[26] Schachinger E, Carbotte JP. Coupling to spin fluctuations from conductivity scattering rates. Phys Rev B. 2000; 62(13): 9054-9058.

[27] Guyard W, Sacuto A, Cazayous M, Gallais Y, Le Tacon M, Colson D, *et al*. Temperature dependence of the gap size near the Brillouin-zone nodes of $HgBa_2CuO_{4+\delta}$ superconductors. Phys Rev Lett. 2008; 101(9): 097003-097006.

[28] Fedorov AV, Valla T, Johnson PD, Li Q, Gu GD, Koshizuka N. Temperature dependent photoemission studies of optimally doped $Bi_2Sr_2CaCu_2O_8$. Phys Rev Lett. 1999; 82(10): 2179-2182.

[29] Ideta S, Takashima K, Hashimoto M, Yoshida T, Fujimori A, Anzai H, *et al*. Enhanced superconducting gaps in the trilayer high-temperature $Bi_2Sr_2Ca_2Cu_3O_{10+\delta}$ cuprate superconductor. Phys Rev Lett. 2010; 104(22): 227001-227004.

[30] Yoshida T, Hashimoto M, Ideta S, Fujimori A, Tanaka K, Mannella N, *et al*. Universal versus material-dependent two-gap behaviors of the high-T_c cuprate superconductors: Angle-resolved photoemission study of $La_{2-x}Sr_xCuO_4$. Phys Rev Lett. 2009; 103(3): 037004-037007.

[31] Kurihara S. Interacting hole-spin model for oxide superconductors. Phys Rev B. 1989; 39(10): 6600-6606.

[32] Chubukov AV, Morr DK. Electronic structure of underdoped cuprates. Phys Rep. 1997; 288(1-6): 355-387.

[33] Cho JH, Borsa F, Johnston DC, Torgeson DR. Spin dynamics in $La_{2-x}Sr_xCuO_4$ ($0.02 \le x \le 0.08$) from La139 NQR relaxation: Fluctuations in a finite-length-scale system. Phys Rev B. 1992; 46(5): R3179-R3182.

[34] Kitazawa A. Electronic structures of oxide superconductors – Development of concepts. Earlier and Recent Aspects of Superconductivity, Edited by Bednorz JG and Müller KA. 1991; 45-65.

[35] Tranquada JM. Magnetic and electronic correlations in $YBa_2Cu_3O_{6+x}$. Earlier and Recent Aspects of Superconductivity, Edited by Bednorz JG and Müller KA. 1991; 422-440.

[36] Germain P, Labbé J. Orthorhombicity, anitiferromagnetism and superconductivity in $YBa_2Cu_3O_{6+x}$. Europhys Lett. 1993; 24(5): 391-396.

[37] Burger JP, Zanoun Y. Main properties and origin of the new high-T_c superconductors. Materials Chemistry and Physics. 1992; 32(1): 177-182.

[38] Barford W, Gunn JMF. The theory of the measurement of the London penetration depth in uniaxial type II superconductors by muon spin rotation. Physica C. 1988; 156(4): 515-522.

[39] Keller H. Muon spin rotation experiments in high-T_c superconductors. Earlier and Recent Aspects of Superconductivity, Edited by Bednorz JG and Müller KA. 1991; 222-239.

[40] Pokrovsky VL. Physical effects in layered superconductors. Phys Rep. 1997; 288(1-6): 325-345.

[41] Ekino T, Akimitsu J. Energy gaps in Bi-Sr-Ca-Cu-O and Bi-Sr-Cu-O systems by electron tunneling. Phys Rev B. 1989; 40(10): 6902-6911.

[42] Kadowaki K, Li JN, Franse JJM. Superconducting fluctuation effects on the magnetoconductivity in single-crystalline $YBa_2Cu_3O_{7-\delta}$ and $Bi_2Sr_2CaCu_2O_{8+\delta}$. J Magn Magn Mater. 1990; 90-91: 678-680.

[43] Panagopoulos C, Cooper JR, Peacock GB, Gameson I, Edwards PP, Schmidbauer W, *et al*. Anisotropic magnetic penetration depth of grain-aligned $HgBa_2Ca_2Cu_3O_{8+\delta}$. Phys Rev B. 1996; 53(6): R2999-R3002.

[44] Abrikosov AA, Campuzano JC, Gofron K. Experimentally observed extended saddle point singularity in the energy spectrum of YBa2Cu3O6.9 and YBa2Cu4O8 and some of the consequences. Physica C. 1993; 214(1-2): 73-79.

[45] Ding H, Campuzano JC, Gofron K, Gu C, Liu R, Veal BW, *et al*. Gap anisotropy in $Bi_2Sr_2CaCu_2O_{8+\delta}$ by ultrahigh-resolution angle-resolved photoemission. Phys Rev B. 1994; 50(2): 1333-1336.

[46] Ma J. Quitmann C, Kelley RJ, Alméras P, Berger H, Margaritondo G, *et al*. Observation of a van Hove singularity in $Bi_2Sr_2CaCu_2O_{8+x}$ with angle-resolved photoemission. Phys Rev B. 1995; 51(6): 3832-3839.

[47] Dessau DS, Shen Z-X, King DM, Marshall DS, Lombardo LW, Dickinson PH, *et al*. Key features in the measured band structure of $Bi_2Sr_2CaCu_2O_{8+\delta}$: Flat bands at E_F and Fermi surface nesting. Phys Rev Lett. 1993; 71(17): 2781-2784.

[48] Newns DM, Tsuei CC, Pattnaik PC, Kane CL. Cuprate superconductivity: The van Hove scenario. Comments Condens Matter Phys. 1992; 15: 273-302.

[49] Newns DM, Tsuei CC, Huebener RP, van Bentum PJM, Pattnaik PC, Chi CC. Quasiclassical transport at a van Hove singularity in cuprate superconductors. Phys Rev Lett. 1994; 73(12): 1695-1698.

[50] Houssa M, Ausloos M, Cloots R. Thermal conductivity of $YBa_2(Cu_{1-x}Zn_x)_3O_{7-\delta}$: Relation between x and δ. Phys Rev B. 1997; 56(10): 6226-6230.

[51] Schulz HJ. Superconductivity and antiferromagnetism in the two-dimensional Hubbard model: Scaling theory. Europhys Lett. 1987; 4(5): 609-615.

[52] Xing DY, Liu M, Gong CD. Comment on "Anomalous isotope effect and van Hove singularity in superconducting Cu oxides". Phys Rev Lett. 1992; 68(7): 1090.

[53] Bechlaghem A, Bourbie D. Properties of the superconducting gap ratio in the van Hove scenario of high-T_c oxides. Mod Phys Lett B. 2010; 24(23): 2395-2401.

[54] Bechlaghem A, Bourbie D. Theory of the isotope effect and superconducting transition temperature in high-T_c oxides. Mod Phys Lett B. 2011; 25(26): 2069-2078.

[55] Bechlaghem A, Bourbie D. Isotope effect due to the super-exchange interaction and van Hove singularity in high-T_c superconductors. J App Phys. 2013; 114(6): 063901-063903.

[56] Bok J, Bouvier J. Superconductivity in cuprates, the van Hove scenario. J Supercond. 1999; 12(1): 27-31.

[57] Novikov DL, Gubanov VA, Freeman AJ. Electronic structure and Fermi surface topology of the infinite-layered superconductor $Sr_{1-x}Ca_xCuO_2$. Physica C. 1993; 210(3-4): 301-307.

[58] Udomsamuthirun P, Yoksan S, Crisan M. Effect of orthorhombic distortion and second-nearest neighbor hopping on gap-to T_c ratio. J Supercond. 1997; 10(3): 189-191.

[59] Cappelluti E, Pietronero L. Nonadiabatic superconductivity: The role of van Hove singularities. Phys Rev B. 1996; 53(2): 932-944.

[60] Labbé J, Bok J. Superconductivity in alkaline-earth-substituted La_2CuO_4: a theoretical model. Europhys Lett. 1987; 3(11): 1225-1230.

[61] Markiewicz RS. Van Hove excitons and high-T_c superconductivity VIIIA: Valence bond density waves. Physica C. 1992; 193(3-4): 323-343.

[62] Markiewicz RS. Van Hove excitons and high-T_c superconductivity VIIIB. vHs - Jahn-Teller effect. Physica C. 1992; 200(1-2): 65-91.

[63] Markiewicz RS. Is the pseudogap in the high-T_c cuprates evidence for dynamic van Hove Jahn-Teller effects? J Supercond. 1995; 8(5) 579-582.

[64] Markiewicz RS. Van Hove Jahn-Teller effect and high-T_c superconductivity. J Physics and Chemestry of Solids. 1993; 54(10): 1153-1156.

[65] Apostol M. On the mechanism of high-temperature superconductivity in Ba-La(Y)-Cu-O type systems. Int J Mod Phys B. 1987; 1(3-4): 957-964.

[66] Apostol M, Popescu M. The relation between the critical temperature and the oxygen content of the superconducting phase $YBa_2Cu_3O_z$. Phyl Mag Lett. 1988; 57(6): 305-309.

[67] Apostol M, Vasiliu-Doloc L. High-temperature superconductivity from electron-lattice coupling. Int J Mod Phys B. 1992; 6(9): 1539-1559.

[68] Liu FH, Apostol M. Critical temperature, isotope effect and superconducting gap in the $M_xLa_{2-x}CuO_4$ and $M_2RCu_3O_{7-\delta}$-type superconductors. Int J Mod Phys B.1988; 2(6): 1415-1429.

[69] Apostol M. On the high temperature superconductivity in 124-class of superconductors. Mod Phys Lett B. 1989; 3(11) 847-852.

[70] Vasiliu L, Apostol M. On the high-temperature superconductivity of $Sr_xLa_{2-x}CuO_{4-\delta}$. J Supercond. 1989; 2(4) 513-528.

[71] Apostol M, Buzatu F, Liu FH. Critical temperature of third generation high-temperature superconductors. Int J Mod Phys B. 1990; 4(1): 159-177.

[72] Aoki H, Kamimura H. Jahn-Teller-effect mediated superconductivity in oxides. Solid State Commun. 1987; 63(7): 665-669.

[73] Johnson KH, Clougherty DP, McHenry ME. Dynamic Jahn-Teller coupling anharmonic oxygen vibrations and high-T_c superconductivity in oxides. Mod Phys Lett B. 1989; 3(18): 1367-1374.

[74] Englman R, Halperin B, Weger M. Jahn-teller (reverse sign) mechanism for superconductive pairing. Physica C. 1990; 169(3-4): 314-324.

[75] Fil DV, Tokar OI, Shelankov AL, Weber W. Lattice-mediated interaction of Cu^{2+} Jahn-Teller ions in insulating cuprates. Phys Rev B. 1992; 45(10): 5633 –5640.

[76] Force L, Bok J. Superconductivity in two dimensional systems: van Hove singularity and Coulomb repulsion. Solid State Commun. 1993; 85(11): 975-978.

[77] Getino JM, de Llano M, Rubio H. Properties of the gap energy in the van Hove scenario of high-temperature superconductivity. Phys Rev B. 1993; 48(1): 597-599.

[78] Tsuei CC, Newns DM, Chi CC, Pattnaik PC. Anomalous isotope effect and van Hove singularity in superconducting Cu oxides. Phys Rev Lett. 1990; 65(21): 2724-2727.

[79] Bechlaghem A, Mostéfa M, Zanoun Y. Gap energy, isotope effect and coherence length in high-T_c oxides. Int J Mod Phys B. 1999; 13(32): 3915-3925.

[80] Sherman A, Schreiber M. Normal-state pseudogap in the spectrum of strongly correlated fermions. Phys Rev B. 1997; 55(2): R712-R715.

[81] Loeser AG, Shen Z-X, Dessau DS, Marshall DS, Park CH, Fournier P, *et al*. Excitation gap in the normal state of underdoped $Bi_2Sr_2CaCu_2O_{8+\delta}$. Science. 1996; 273(5273): 325-329.

[82] Shen Z-X, Spicer WE, King DM, Dessau DS, Wells BO, *et al*. Photoemission studies of high-T_c superconductors: The superconducting gap. Science. 1995; 267(5196): 343-350.

[83] Williams GVM, Tallon JL, Haines EM, Michalak R, Dupree R. NMR evidence for a d-wave normal-state pseudogap. Phys Rev Lett. 1997; 78(4): 721-724.

[84] Williams GVM, Haines EM, Tallon JL. Pair breaking in the presence of a normal-state pseudogap in high-T_c cuprates. Phys Rev B. 1998; 57(1): 146-149.

[85] Tsuei CC, Kirtley JR, Chi CC, Yu-Jahnes LS, Gupta A, Shaw T, *et al*. Pairing symmetry and flux quantization in a tricrystal superconducting ring of $YBa_2Cu_3O_{7-\delta}$. Phys Rev Lett. 1994; 73(4): 593-596.

[86] Khasanov R, Shengelaya A, Maisuradze A, Mattina LF, Bussmann-Holder A, Keller H, *et al*. Experimental evidence for two gaps in the high-temperature $La_{1.83}Sr_{0.17}CuO_4$ superconductor. Phys Rev Lett. 2007; 98(5): 057007-057010.

[87] Deutscher G. Andreev–Saint-James reflections: A probe of cuprate superconductors. Rev Mod Phys. 2005; 77(1): 109-135.

[88] Brandaw B. Characteristic features of the exotic superconductors. Phys Rep. 1998; 296(1): 1-63.

[89] Bok J, Force L. Origin of superconductivity in cuprates: The van Hove scenario. Physica C. 1991; 185-189(3): 1449-1450.

[90] Bardeen J, Cooper LN, Schrieffer JR. Theory of superconductivity. Phys Rev 1957; 108: 1175-1204.

[91] Kresin VZ, Wolf SA, Ovchinnikov YN. Exotic normal and superconducting properties of the high-T_c oxides. Phys Rep. 1997; 288(1-6): 347-354.

[92] Mook HA, Yethiraj M, Aeppli G, Mason TE, Armstrong T. Polarized neutron determination of the magnetic excitations in $YBa_2Cu_3O_7$. Phys Rev Lett. 1993; 70(22): 3490-3493.

[93] Rossat-Mignod J, Regnault LP, Vettier C, Bourges P, Burlet P, Bossy J, *et al*. Neutron scattering study of the $YBa_2Cu_3O_{6+x}$ system. Physica C. 1991; 185-189(1): 86-92.

[94] Szczesniak R, Mierzejewski M, Zielinski J, Entel P. Modification of the isotope effect by the van Hove singularity of electrons on a two-dimensional lattice. Solid State Commun. 2001; 117(1): 369-371.

[95] Szczesniak R, Dyga M. The van Hove singularity and two-dimensional charge density waves. Exact analytical results. Acta Physica Slovaca. 2003; 53(6): 477-487.

[96] Balseiro CA, Falicov LM. Superconductivity and charge-density waves. Phys Rev B. 1979; 20(11): 4457-4464.

[97] Yndurain F. Model for the variation upon doping of the isotope coefficient in high-T_c superconductors. Phys Rev B. 1995; 51(13): 8494-8497.

[98] Gupta HC. Electron-phonon interaction for an analytic solution to the BCS equation for the high temperature superconductors. Mod Phys Lett B. 1991; 5(20): 1349-1353.

[99] Sarkar S, Das AN. Isotope-shift exponent, pressure coefficient of T_c, and the superconducting-gap ratio within the van Have scenario. Phys Rev B. 1994; 49(18): 13070-13074.

[100] Bouvier J, Bok J. Gap anisotropy and van Hove singularities in high-T_c superconductors. Physica C. 1995; 249(1): 117-122.

[101] Ratanaburi S, Udomsamuthirun P, Yoksan S. Ratio $2\Delta_0/k_bT_c$ in a van Hove superconductor. J Supercond. 1996; 9(5): 485-486.

[102] Krunavakarn B, Udomsamuthirun P, Yoksan S, Grosu I, Crisan M. The gap-to-T_c ratio of a van Hove superconductor. J Supercond. 1998; 11(2): 271-273.

[103] Pakokthom C, Krunavakarn B, Udomsamuthirun P, Yoksan S. Reduced-gap ratio of high-T_c cuprates within the *d*-wave two-dimensional van Hove scenario. J Supercond. 1998; 11(4): 429-432.

[104] Das AN, Lahiri J, Sil S. Superconducting gap ratio and isotope-shift exponent in a pair-tunneling model. Physica C. 1998; 294(1-2): 97-104.

[105] Kaskamalas S, Krunavakarn B, Rungruang P, Yoksan S. Dependence of the gap ratio on the Fermi level shift in a van Hove superconductor. J Supercond Incorp Novel Mag. 2000; 13(1): 33-36.

[106] Gabovich AM, Voitenko AI, Ekino T, Li MS, Szymczak H, Pekała M. Competitionof superconductivity and charge density waves in cuprates: Recent evidence and interpretation. Advances in Condensed Matter Physics. 2009; 2010(1): 681070-109.

[107] Croft TP, Lester C, Senn MS, Bombardi A, Hayden SM. Charge density wave fluctuations in $La_{2-x}Sr_xCuO_4$ and their competition with superconductivity. Phys Rev B. 2014; 89(22): 224513-520.

[108] Torchinsky DH, Mahmood F, Bollinger AT, Božović I, Gedik N. Fluctuating charge-density waves in a cuprate superconductor. Nature Materials. 2013; 12(1): 387-391.

[109] Chang J, Blackburn E, Holmes AT, Christensen NB, Larsen J, Mesot J, *et al*. Direct observation of competition between superconductivity and charge density wave order in $YBa_2Cu_3O_{6.67}$. Nature Phys. 2012; 8(1): 871-876.

[110] Panda SK, Rout GC. Interplay of CDW, SDW and superconductivity in high-T_c Cuprates. Physica C. 2009; 469(13): 702-706.

Received on 23-06-2014 Accepted on 14-07-2014 Published on 28-08-2014

http://dx.doi.org/10.15379/2408-977X.2014.01.01.3

© 2014 A. Bechlaghem; Licensee Cosmos Scholars Publishing House.
This is an open access article licensed under the terms of the Creative Commons Attribution Non-Commercial License (http://creativecommons.org/licenses/by-nc/3.0/), which permits unrestricted, non-commercial use, distribution and reproduction in any medium, provided the work is properly cited.